Chemistry–A European Journal

Communication
doi.org/10.1002/chem.202003492

Supported Catalysts | *Hot Paper* |

Facile Synthesis of Size-Controlled Nitrogen-Doped Mesoporous Carbon Nanosphere Supported Ultrafine Ru Nanoparticles for Selective Hydrogenation of Quinolines

Zhengbin Tian+,[b, c] Haibin Jiang+,[a, b] Minghua Huang,*[a] and Guang-Hui Wang*[b, c]

Abstract: Nitrogen-doped mesoporous carbon nanosphere (NMCS) with tunable sizes and uniform mesoporosity was synthesized by a facile soft-templating method. During the synthesis, F127 (PEO–PPO–PEO triblock copolymer) could be used not only as a soft template to generate the mesostructure but also as a size-control agent to tailor the size of NMCS in a relatively wide range of 100 to 700 nm. In addition, the synthesis process was simple and suitable for large-scale production. Moreover, the NMCS was used as support of ultrafine Ru nanoparticles (Ru/NMCS), which exhibited good catalytic performances for selective hydrogenation of quinolones. It is expected that the simple synthetic strategy for the NMCS can generate extensive interest in many catalysis and sorption applications.

Nitrogen-doped mesoporous carbons (NMCs) have attracted much attention in various applications, such as supercapacitors, batteries, and catalysis, due to their unique properties of mesoporous structure (leading to high surface area, large pore volume, etc.) and nitrogen-doped carbon framework (improved basicity and enhanced π-donor capability).[1–4] In catalysis, the NMCs exhibit outstanding advantages as catalyst supports, where the mesoporous structure allows efficient mass transfer during catalysis, while the nitrogen in the carbon framework can help to stabilize the supported active species and even modify their chemical and electronic structure to achieve specific catalytic properties.[5,6] For example, many NMC-supported catalysts with various active species, including metal/metal oxide nanoparticles, metal phosphides/carbides, and isolated single atoms, have been synthesized successfully, which in most cases exhibit high activity, excellent selectivity, and good stability in catalytic reactions.[6–11]

Besides the active species, design of NMCs with different features is also one of the key topics for the synthesis of supported catalysts with enhanced catalytic performance. Especially, spherical NMC (NMCS) with tunable size is an ideal catalyst support due to the uniform morphology, highly accessible mesochannels, etc.[12,13] In general, there are two main methods to fabricate the NMCS: (1) post-treatment of the presynthesized mesoporous carbon nanospheres (MCS) by N-containing reagents such as NH_3, urea, melamine, nitric acid, and amines;[14] (2) direct synthesis of NMCS by using N-containing chemicals as both carbon and nitrogen precursors (such as 3-aminophenol, aniline, dopamine, melamine-formaldehyde, pyrrole, polyacrylonitrile, etc.) via hard- or soft-templating strategies, where the N atoms can be directly doped into the carbon skeleton, not just on the surface.[15,16]

Although the former is suitable for large-scale synthesis, it often yields NMCS with non-uniform doping of nitrogen and unstable mesostructure. The hard-templating strategy in the later method involves employing nanosized mesoporous sphere (usually silica) as a template to synthesize the NMCS. However, this strategy often suffers from the drawbacks of massive use of the templates and template removal processes, leading to low production efficiency and high cost. In addition, the morphology, mesopore size, and diameter of the replicated NMCS are always limited by the used template, leading to poor ability in adjusting the structures of NMCS.[17,18] In contrast, the soft-templating strategy in the later method involves co-assembling the N-containing precursors with surfactants (normally triblock copolymers, e.g., Pluronic P123 and F127) to generate the mesostructured polymer spheres, followed by pyrolysis to obtain the NMCS. From the perspective of material synthesis, this is the simplest method to synthesize the NMCS, where the structural features of NMCS can be easily tailored by changing the synthesis parameters (e.g., temperature, solvent, pH, concentration of precursors, etc.) of co-assembling process.[19,20] Therefore, direct synthesis of NMCS with tunable sizes via soft-templating strategy is highly attractive for scale-up production and application in catalysis.

Herein, we develop a facile soft-templating method for directly synthesizing the NMCS with tunable sizes using 3-amino-

---

[a] H. Jiang,+ Prof. M. Huang
School of Materials Science and Engineering
Ocean University of China
Qingdao 266100 (P. R. China)
E-mail: huangminghua@ouc.edu.cn

[b] Z. Tian,+ H. Jiang,+ Prof. G.-H. Wang
Key Laboratory of Biofuels
Qingdao Institute of Bioenergy and Bioprocess Technology
Chinese Academy of Sciences
Qingdao, 266101 (P. R. China)
E-mail: wanggh@qibebt.ac.cn

[c] Z. Tian,+ Prof. G.-H. Wang
University of Chinese Academy of Sciences
Beijing, 100049 (P. R. China)

[+] These authors contributed equally to this work.

Supporting information and the ORCID identification number(s) for the author(s) of this article can be found under: https://doi.org/10.1002/chem.202003492.

phenol (3-AP) as carbon and nitrogen sources and F127 (PEO–PPO–PEO triblock copolymer) as a surfactant. The method is simple and easy to operate, involving just two steps: a polymerization process and a subsequent pyrolysis process (Scheme 1). The NMCS sizes could be simply tailored in a relatively wide range of 100 to 700 nm by changing the used amount of F127. The large-scale production could be realized by scaling up the polymerization process. Next, the Ru ions are easily introduced into the framework of the as-obtained NMCS due to their interaction with the nitrogen species in the NMCS. After H_2 reduction, the catalyst of Ru/NMCS with ultrafine Ru nanoparticles is obtained, which shows good catalytic performances for selective hydrogenation of quinolines.

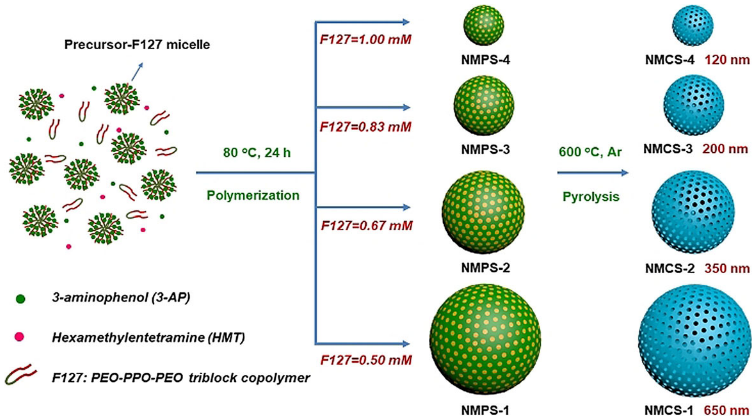

Scheme 1. Schematic illustration of the synthesis of NMCS with tunable sizes.

In the polymerization process, 3-AP, hexamethylenetetramine (HMT), and F127 are dissolved in water to form the mixed solution, where the 3-AP and HMT (HMT can decompose into formaldehyde and ammonia) are used as polymer precursors and F127 is used as surfactant. The formaldehyde generated from HMT can polymerize with 3-AP in the presence of F127 to form the nitrogen-doped mesostructured polymer nanospheres. After stirring at 80 °C for 24 h, the nitrogen-doped mesostructured polymer nanospheres (denoted as NMPS-*x*, where the number of *x* represents the synthesis with different amount of F127, Table S1) are obtained, which can be converted into NMCS-*x*-*T* (*T* represents the pyrolysis temperature) after pyrolysis under Ar atmosphere. Our method is different from the synthesis system reported by Wang et al.,[21] where the morphology and the size of NMCS (tailoring in the range of 90 to 220 nm) could be well controlled by adding additional ammonia in the 3-AP/HMT/F127 system (in absence of ammonia, only products with irregular morphology and uneven sizes were obtained). In our case, the NMCS with spherical morphology and uniform size can be synthesized without adding ammonia; in addition, by simply changing the used amount of F127, the size of NMCS can be well tailored in a relatively wide range of 100 to 700 nm. Moreover, the method could achieve a good yield; for example, approximately 0.9 g of NMPS-1 was prepared after polymerization in one batch (Table S1), and large-scale product could be obtained by scaling up the polymerization process.

The morphologies and mesostructures of the NMCS-*x*-600 with tunable sizes are characterized by scanning electron microscopy (SEM) and transmission electron microscopy (TEM). As shown in Figure 1 a,b, the NMCS-1-600 (F127 concentration during synthesis is 0.5 mM) has a spherical-like morphology with size of 650 nm, and the TEM image shown in Figure 1 c indicates that the NMCS-1-600 is mesostructured, which is conducive to efficient mass transfer during catalytic reactions.[22] Increasing the F127 concentration to 0.67, 0.83, and 1.00 mM, the NMCS products (Figure 1 d-l) have similar morphology and mesostructure as NMCS-1-600; however, the size gradually decreases to 350 nm for NMCS-2-600, 200 nm for NMCS-3-600, and 120 nm for NMCS-4-600, respectively. These results indicate that the F127 can be used not only as a soft template to generate the mesostructure, but also as a size-control agent to tailor the size of NMCS. It can be explained that increasing the F127 concentration can facilitate the formation of more resol-F127 micelles at the beginning of polymerization, resulting in the generation of more nuclei and thus decreasing the size of NMCS.[21]

The porous textures of these NMCS products are characterized by N_2 sorption measurements. The N_2

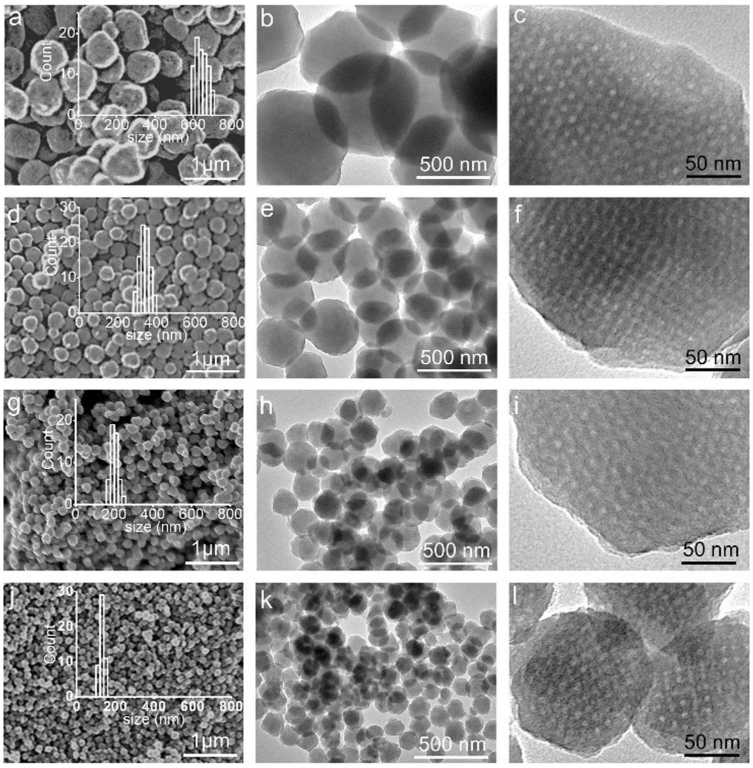

Figure 1. SEM and TEM images of (a–c) NMCS-1-600, (d–f) NMCS-2-600, (g–i) NMCS-3-600, and (j–l) NMCS-4-600.

sorption isotherms of all NMCS products (Figure 2a) exhibit steep uptakes at relative pressure $P/P_0 < 0.1$, indicating the existence of microporosity, and hysteresis loops in the $P/P_0 \approx 0.35$–0.70 range, suggesting the uniform mesoporosity. For the samples of NMCS-2–600, NMCS-3-600, and NMCS-4-600, obvious hysteresis loops at relative pressure $P/P_0 > 0.90$ are observed, which can be attributed to the interparticle condensation because of their relatively small particle size.[22] The pore sizes of these products (Figure 2b) slightly decrease from 5.5 nm (NMCS-1-600) to 4.8 nm (NMC-2-600), 4.3 nm (NMCS-3-600), and 4.0 nm (NMCS-4-600), along with the decreasing of particle size. According to the Brunauer–Emmett–Teller (BET) method, the specific surface areas (S_{BET}) of these NMCS products are very similar, which are in the range of 434 to 476 $m^2 g^{-1}$ (Table S2). The total pore volumes of the NMCS products are also nearly identical, approximately 0.32 $cm^3 g^{-1}$ (Table S2). In addition, according to the elemental analysis by sample combustion, the amounts of bulk nitrogen in these products are approximately 9.2–9.5 wt% (Table S2).

X-ray photoelectron spectroscopy (XPS) is employed to study the surface chemistry properties of these NMCS products. Taking the samples of NMCS-3-*T* (pyrolysis at temperature ranging from 360 to 1000 °C) as examples, the scan survey XPS spectra show the presence of carbon, oxygen, and nitrogen (Figure 2c). In the N 1s region (Figure 2d), the spectrum of NMCS-3–360 exhibits three peaks that can be attributed to pyridinic nitrogen (398.4 eV), amino group (399.6 eV), and pyrrolic nitrogen (400.4 eV), respectively. The existence of amino group may be caused by incomplete decomposition of 3-AP during pyrolysis at 360 °C. Increasing the pyrolysis temperature to 600 °C, the peak attributed to amino group vanishes and only two peaks attributed to pyridinic (398.4 eV) and pyrrolic nitrogen (400.4 eV) are exhibited in the N 1s spectrum of NMCS-3-600.[23] Further increasing pyrolysis temperature to 800 and 1000 °C, the N species are quite complex, where the N 1s spectra are deconvoluted into five peaks that can be assigned to nitride (397.9 eV), amine (399.1 eV), pyridonic nitrogen (400.8 eV), probably quaternary nitrogen (401.9 eV), and pyridine-*N*-oxide (403.3 eV).[3] In addition, according to the XPS data, the amounts of surface nitrogen are 3.8 wt% for NMCS-3-360, 6.1 wt% for NMCS-3-600, 2.5 wt% for NMCS-3-800, and 1.8 wt% for NMCS-3-1000, respectively.

Then, the NMCS-3-600 is chosen as an example support for Ru nanoparticles, whereby the Ru ions are adsorbed onto the surface of NMCS-3-600 due to their coordination with the surface N-species,[24,25] followed by H_2 reduction to generate the

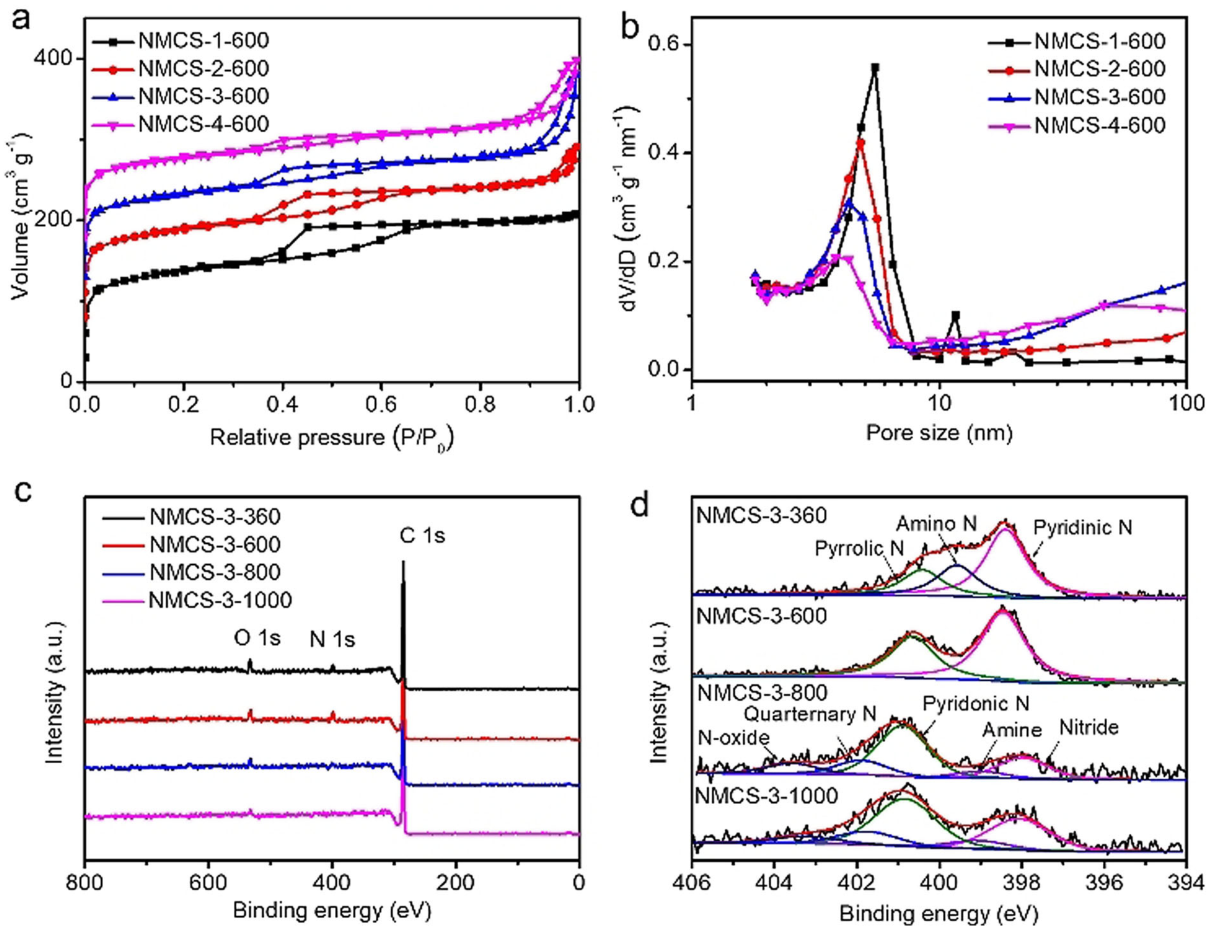

Figure 2. (a) N_2 sorption isotherms of NMCS-1-600, NMCS-2-600 (shifted vertically by 50 $cm^3 g^{-1}$), NMCS-3-600 (100 $cm^3 g^{-1}$), and NMCS-4-600 (150 $cm^3 g^{-1}$) and (b) their corresponding pore size distributions. (c) Scan survey XPS spectra and (d) N 1s spectra of NMCS-3-360, NMCS-3-600, NMCS-3-800, and NMCS-3-1000.

supported Ru catalyst (Ru/NMCS-3-600). The high-angle annular dark field scanning transmission electron microscopy (HAADF-STEM) image (Figure 3a) shows that ultrafine Ru nanoparticles (1–2 nm) are formed and uniformly dispersed on NMCS-3-600. The X-ray diffraction (XRD) pattern of Ru/NMCS-3-600 (Figure 3b) exhibits only two broad peaks at around 24 and 43°, both of which could be assigned to the amorphous carbon.[26] The broad peak centered at 43° could also be assigned to the Ru nanoparticles, which have smaller particle size. This result indicates that no large Ru nanoparticles are formed on the NMCS-3-600, which is in line with the observed results from TEM and STEM images (Figure 3a, Figure S1). The formation of ultrafine Ru nanoparticles on NMCS-3-600 can be attributed to the coordination between Ru ions and the surface N-species.

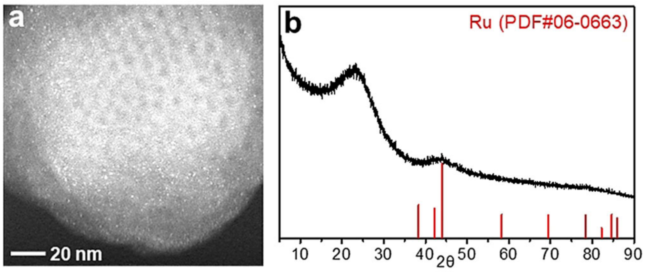

Figure 3. (a) XRD pattern and (b) HAADF-STEM image of as-prepared Ru/NMCS-3-600.

The selective hydrogenation of quinolines to produce 1,2,3,4-tetrahydroquinolines is very important in the fields of pharmaceuticals, agrochemicals, and other fine chemicals.[27,28] Therefore, the catalytic performance of Ru/NMCS-3-600 was investigated by hydrogenation of quinolines. First, hydrogenation of quinoline without catalyst was performed at 100 °C with 3.5 MPa H_2 pressure; no reaction occurred after 6 h (Table 1, entry 1). When using pure NMCS-3-600 as catalyst, only a low conversion (< 2%) was observed (Table 1, entry 2). However, when using Ru/NMCS-3-600 as the catalyst, over 99% conversion and 98% selectivity towards the target product were obtained after 6 h under the same conditions (Table 1, entry 3). Extending the reaction time to 9 h, the selectivity of target product was still higher than 95% (Table 1, entry 4). The excellent performance of Ru/NMCS-3-600 for selective hydrogenation of quinolone may be due to the small Ru nanoparticles and the existence of N-species that can tailor the electric property of Ru nanoparticles.[27] In addition, the N-species in the Ru/NMCS-3-600 can also enhance the selective adsorption of the N-heterocycle of quinolone through hydrogen-bond interactions, thus accelerating the hydrogenation of N-heterocycle ring but preventing further hydrogenation of aromatic ring.[29] In contrast, when using carbon black (Vulcan XC-72, without N-species) as support, the Ru nanoparticles with a broad size distribution are formed and unevenly dispersed on the Vulcan XC-72 (Ru/XC-72, synthesized via the impregnation method, Figure S2). Over the Ru/XC-72, 99% conversion of quinolone was achieved, but only with 69% selectivity towards the target product (Table 1, entry 5), which probably due to the absence of N-species and/or the presence of large Ru nanoparticles in the Ru/XC-72. Therefore, the Ru/NMCS-3-600 with nitrogen doping and ultrafine Ru nanoparticles is an excellent catalyst for selective hydrogenation of quinolones.

Table 1. Selective hydrogenation of quinolines.[a]

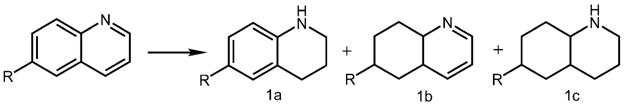

Entry	Catalyst	Substrate	Conv. [%]	Select. [%] 1a	1b	1c
1	–	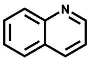	–	–	–	–
2	NMCS-3-600		< 2	–	–	–
3	Ru/NMCS-3-600		99	> 98	< 2	0
4[b]	Ru/NMCS-3-600		99	95	< 1	4
5	Ru/XC-72		99	69	–	31
6	Ru/NMCS-3-600	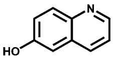	99	> 99	< 1	0
7	Ru/NMCS-3-600	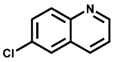	99	> 99	< 1	0
8	Ru/NMCS-3-600	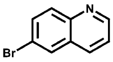	99	> 99	< 1	0
9[c]	Ru/NMCS-3-600	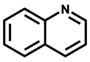	99	> 98	< 2	0

[a] Reaction conditions: 50 mg catalyst, 1 mmol substrate, 5 mL solvent, 100 °C, 3.5 MPa H_2, 6 h; [b] Reaction time: 9 h; [c] Result of the fifth cycle.

Moreover, hydrogenation of other three quinolones over the Ru/NMCS-3-600 was also studied under the same conditions. In the case of 6-hydroxyquinoline, 99% conversion and 99% selectivity are achieved without detecting any over-reduced products (Table 1, entry 6). Usually, the selective hydrogenation of halogen (e.g., Cl and Br) substituted quinolines is challenging due to the easy formation of the dehalogenated and over-hydrogenated byproducts.[27] Impressively, such substrates were completely converted into the halogenated 1,2,3,4-tetrahydroquinolines over the Ru/NMCS-3-600 without producing byproducts (Table 1, entries 7 and 8), demonstrating the general applicability of Ru/NMCS-3-600 for efficient selective hydrogenation of quinolines. In addition, the recycling stability of Ru/NMCS-3-600 was tested in the hydrogenation of quinolone; the catalyst still retained the good activity without changing the selectivity towards 1,2,3,4-tetrahydroquinoline after five runs (Table 1, entry 9), suggesting the excellent stability of Ru/NMCS-3-600.

In summary, we have developed a facile soft-templating method for synthesizing NMCS with tunable sizes. In this method, F127 plays two important roles: acting as a soft template to generate the uniform mesoporosity and as surfactant to tailor the NMCS size in a relatively wide range of 100 to 700 nm. The NMCS are fully characterized by TEM, SEM, XPS, and N_2 sorption, providing a systematical comparison for different NMCS-*x*-*T*. In addition, ultrafine Ru nanoparticles are supported on the NMCS-3-600 with the help of N-species, which displays superior catalytic performance for hydrogenation of various quinolines with $>99\%$ conversion and $>98\%$ selectivity towards the target products. It is expected that the simple synthetic strategy for the NMCS with tunable sizes will generate extensive interest in many catalysis and sorption applications.

Acknowledgements

This work was supported by the National Natural Science Foundation of China (21872159 and 21775142), QIBEBT (QIBEBT ZZBS201802) and the DNL Cooperation Fund, CAS (DNL180402).

Conflict of interest

The authors declare no conflict of interest.

Keywords: hydrogenation · mesoporous carbon · quinolines · soft templating · tunable sizes

[1] Y. Cao, S. Mao, M. Li, Y. Chen, Y. Wang, *ACS Catal.* **2017**, *7*, 8090–8112.
[2] L. He, F. Weniger, H. Neumann, M. Beller, *Angew. Chem. Int. Ed.* **2016**, *55*, 12582–12594; *Angew. Chem.* **2016**, *128*, 12770–12783.
[3] G. H. Wang, Z. Cao, D. Gu, N. Pfänder, A. C. Swertz, B. Spliethoff, H. J. Bongard, C. Weidenthaler, W. Schmidt, R. Rinaldi, *Angew. Chem. Int. Ed.* **2016**, *55*, 8850–8855; *Angew. Chem.* **2016**, *128*, 8996–9001.
[4] F. Xu, D. Wu, R. Fu, B. Wei, *Mater. Today* **2017**, *20*, 629–656.
[5] C. M. Parlett, K. Wilson, A. F. Lee, *Chem. Soc. Rev.* **2013**, *42*, 3876–3893.
[6] M. B. Gawande, P. Fornasiero, R. Zbořil, *ACS Catal.* **2020**, *10*, 2231–2259.
[7] G. H. Wang, X. Deng, D. Gu, K. Chen, H. Tüysüz, B. Spliethoff, H. J. Bongard, C. Weidenthaler, W. Schmidt, F. Schüth, *Angew. Chem. Int. Ed.* **2016**, *55*, 11101–11105; *Angew. Chem.* **2016**, *128*, 11267–11271.
[8] S. Zhou, L. Shang, Y. Zhao, R. Shi, G. I. Waterhouse, Y. C. Huang, L. Zheng, T. Zhang, *Adv. Mater.* **2019**, *31*, 1900509.
[9] W. Liu, L. Zhang, X. Liu, X. Liu, X. Yang, S. Miao, W. Wang, A. Wang, T. Zhang, *J. Am. Chem. Soc.* **2017**, *139*, 10790–10798.
[10] Y. Pan, K. Sun, S. Liu, X. Cao, K. Wu, W.-C. Cheong, Z. Chen, Y. Wang, Y. Li, Y. Liu, *J. Am. Chem. Soc.* **2018**, *140*, 2610–2618.
[11] J. Meng, J. Li, J. Liu, X. Zhang, G. Jiang, L. Ma, Z.-Y. Hu, S. Xi, Y. Zhao, M. Yan, *ACS Cent. Sci.* **2020**, *6*, 1431–1440.
[12] L. Peng, C.-T. Hung, S. Wang, X. Zhang, X. Zhu, Z. Zhao, C. Wang, Y. Tang, W. Li, D. Zhao, *J. Am. Chem. Soc.* **2019**, *141*, 7073–7080.
[13] Y. Liu, Z. Wang, W. Teng, H. Zhu, J. Wang, A. A. Elzatahry, D. Al-Dahyan, W. Li, Y. Deng, D. Zhao, *J. Mater. Chem. A* **2018**, *6*, 3162–3170.
[14] T.-Y. Ma, L. Liu, Z.-Y. Yuan, *Chem. Soc. Rev.* **2013**, *42*, 3977–4003.
[15] P. Zhang, J. Zhang, S. Dai, *Chem. Eur. J.* **2017**, *23*, 1986–1998.
[16] T. Wang, F. Okejiri, Z. A. Qiao, S. Dai, *Adv. Mater.* **2020**, 2002475.
[17] J. Liu, N. P. Wickramaratne, S. Z. Qiao, M. Jaroniec, *Nat. Mater.* **2015**, *14*, 763–774.
[18] W. Li, J. Liu, D. Zhao, *Nat. Rev. Mater.* **2016**, *1*, 16023.
[19] S. Dutta, A. Bhaumik, K. C.-W. Wu, *Energy Environ. Sci.* **2014**, *7*, 3574–3592.
[20] C. Liang, Z. Li, S. Dai, *Chem. Eur. J.* **2008**, *14*, 3696–3717.
[21] J. Wang, H. Liu, J. Diao, X. Gu, H. Wang, J. Rong, B. Zong, D. S. Su, *J. Mater. Chem. A* **2015**, *3*, 2305–2313.
[22] Y. Fang, D. Gu, Y. Zou, Z. Wu, F. Li, R. Che, Y. Deng, B. Tu, D. Zhao, *Angew. Chem. Int. Ed.* **2010**, *49*, 7987–7991; *Angew. Chem.* **2010**, *122*, 8159–8163.
[23] K. Artyushkova, B. Kiefer, B. Halevi, A. Knop-Gericke, R. Schlogl, P. Atanassov, *Chem. Commun.* **2013**, *49*, 2539–2541.
[24] H. Zhang, P. An, W. Zhou, B. Y. Guan, P. Zhang, J. Dong, X. W. D. Lou, *Sci. Adv.* **2018**, *4*, eaao6657.
[25] Z.-J. Jiang, Z. Jiang, *Sci. Rep.* **2016**, *6*, 27081.
[26] J. Zhang, X. Wang, G. Qi, B. Li, Z. Song, H. Jiang, X. Zhang, J. Qiao, *Carbon* **2016**, *96*, 864–870.
[27] X. Wang, W. Chen, L. Zhang, T. Yao, W. Liu, Y. Lin, H. Ju, J. Dong, L. Zheng, W. Yan, *J. Am. Chem. Soc.* **2017**, *139*, 9419–9422.
[28] W. Gong, Q. Yuan, C. Chen, Y. Lv, Y. Lin, C. Liang, G. Wang, H. Zhang, H. Zhao, *Adv. Mater.* **2019**, *31*, 1906051.
[29] X. Yu, R. Nie, H. Zhang, X. Lu, D. Zhou, Q. Xia, *Microporous Mesoporous Mater.* **2018**, *256*, 10–17.

Manuscript received: July 27, 2020
Revised manuscript received: September 24, 2020
Version of record online: ■■ ■■, 0000

COMMUNICATION

Supported Catalysts

Z. Tian, H. Jiang, M. Huang, G.-H. Wang**

■■–■■

Facile Synthesis of Size-Controlled Nitrogen-Doped Mesoporous Carbon Nanosphere Supported Ultrafine Ru Nanoparticles for Selective Hydrogenation of Quinolines

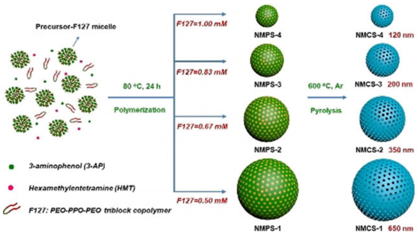

Soft templating: Nitrogen-doped mesoporous carbon nanosphere (NMCS) with tunable sizes and uniform mesoporosity is synthesized by a facile soft-templating method, whereby F127 (PEO–PPO–PEO triblock copolymer) can be used not only as a soft template to generate the mesostructure but also as a size-control agent to tailor the size of NMCS ranging from 100 to 700 nm.